Unraveling the Exciton Quenching Mechanism of Quantum Dots on Antimony-Doped SnO_2 Films by Transient Absorption and Single Dot Fluorescence Spectroscopy

Nianhui Song, Haiming Zhu, Zheng Liu, Zhuangqun Huang, David Wu, and Tianquan Lian*

Department of Chemistry, Emory University, Atlanta, Georgia 30322, United States

ABSTRACT Integrating quantum dots (QDs) into modern optoelectronic devices requires an understanding of how a transparent conducting substrate affects the properties of QDs, especially their excited-state dynamics. Here, the exciton quenching dynamics of core/multishell ($CdSe/CdS_{3ML}ZnCdS_{2ML}ZnS_{2ML}$) quantum dots deposited on glass, tin oxide (SnO_2), and antimony (Sb)-doped tin oxide (ATO) films are studied by transient absorption and single QD fluorescence spectroscopic methods. By comparing ensemble-averaged fluorescence decay and transient absorption kinetics, we show that, for QDs on SnO_2, the exciton is quenched by electron transfer from the QD to SnO_2. At the QD−ATO interface, much faster exciton quenching rates are observed and attributed to fast Auger recombination in charged QDs formed by Fermi level equilibration between the QD and n-doped ATO. Single QDs on SnO_2 and ATO show similar blinking dynamics with correlated fluctuations of emission intensities and lifetimes. Compared to QDs on SnO_2, QDs on ATO films show larger variation of average exciton quenching rates, which is attributed to a broad distribution of the number of charges and nature of charging sites on the QD surface.

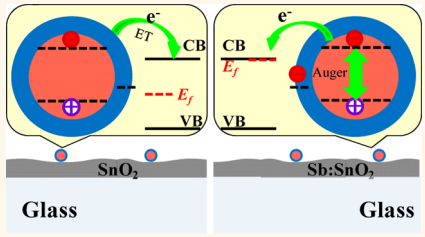

KEYWORDS: blinking dynamics · quantum dots · interfacial charge transfer · charged QDs · single particle spectroscopy · transient absorption spectroscopy

Semiconductor nanocrystals in the quantum-confined size regime, or quantum dots (QDs), have been a subject of intense interest and extensive research in the last three decades. Because of their high absorption cross section over a broad spectral range,[1] tunable electron/hole wavefunctions,[2,3] and size-dependent optical properties,[4] they are considered as promising alternatives to molecular chromophores in various applications ranging from biological imaging[5,6] and light-emitting diodes (LED)[7,8] to photovoltaic and photocatalytic devices.[9−12] In QD-based optoelectronic devices, transparent conducting electrodes (TCE), such as Sn-doped In_2O_3 (ITO), F-doped SnO_2 (FTO), and Sb-doped SnO_2 (ATO), are widely utilized as both windows for light illumination or collection and electrical contact for carrier extraction or injection.[7,8,10,13−16] The presence of TCE and applied external bias was shown to affect exciton dynamics of QDs and modify the single QD blinking dynamics.[17−24] The mechanism by which these changes occur remains unclear.

Because the conduction band edge of the oxide materials (such as In_2O_3 or SnO_2) is lower than that of QDs (*e.g.*, CdSe), electron transfer from excited QDs to the TCE film is energetically favored and has been observed previously.[22,25−28] As shown in Figure 1, n-doping of these materials raises the Fermi levels near their conduction band edges, which also opens up a possible hole transfer pathway for excited QDs in addition to quenching by electron transfer. Furthermore, for QDs on n-doped TCE films, the equilibration of their Fermi levels likely leads to the charging of QDs, which can also affect the exciton dynamics. Previously, we and others reported shortened fluorescence lifetime and suppressed blinking for QDs on n-type ITO films.[19,22,23] We speculated that QDs are charged on n-type ITO due to the electron filling of trapped states and the shortened QD fluorescence lifetime

* Address correspondence to tlian@emory.edu.

Received for review November 23, 2012 and accepted January 2, 2013.

Published online January 02, 2013
10.1021/nn3054494

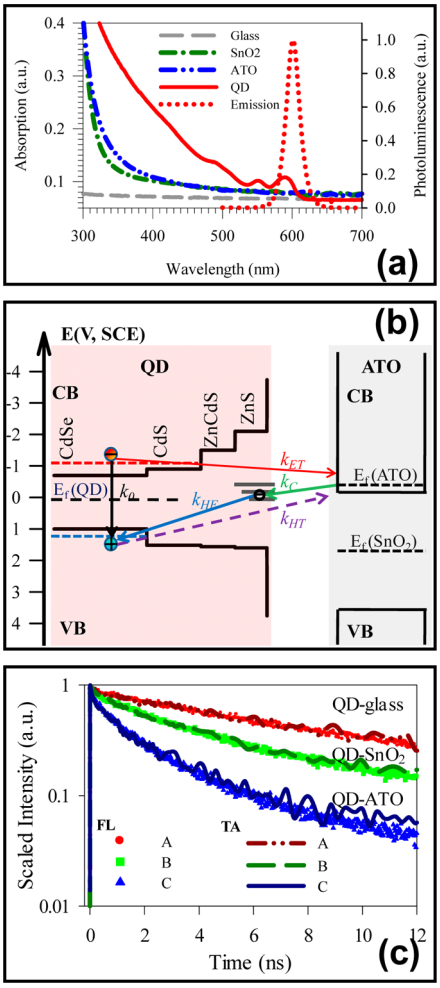

Figure 1. (a) Absorption spectra (left *y*-axis) of a QD colloidal solution (QD, red solid line), sapphire window (gray line), and SnO_2 film (dark green line) and ATO film (blue line) prepared on sapphire windows. Also shown as the red dashed line is the emission spectrum of QDs (right *y*-axis). (b) Schematic diagram of relative energy levels of QD and SnO_2/ATO and possible exciton quenching pathways (see the main text). (c) Transient absorption (TA, solid lines) kinetics at 585 nm (averaged from 581 nm to 690 nm) and ensemble-averaged fluorescence (FL, open symbols) decays of QDs deposited on sapphire windows (A), SnO_2 films (B), and ATO films (C). The TA kinetics have been inverted and normalized for better comparison with the FL kinetics.

can be attributed to Auger recombination of charged QDs and/or exciton quenching by hole transfer to the trapped electron or to ITO.[22] Charging of QDs on the ITO substrate has been experimentally confirmed and quantitatively studied by electrostatic force microscopy by Barnes and co-workers.[23] Guyot-Sionnest and co-workers proposed that, for QDs in contact with ITO, energy transfer between QDs and ITO film is responsible for the observed shortened fluorescence lifetime for the QDs.[19] The same study also reported that electrochemical charging of QDs to form negative trions (exiton + electron) leads to shortened fluorescence lifetime. More recently, electrochemical charging-induced change of QD lifetime and blinking behavior has also been reported, and the role of a midgap trap state was proposed by Klimov and co-workers.[21] These previous studies are based on fluorescence measurement, which on itself is not sufficient to differentiate the multiple pathways (electron transfer, hole transfer, energy transfer, and Auger recombination) for exciton quenching at the QD/ITO interface.

In an effort to reveal the mechanism of exciton quenching at the QD/electrode interface, we report here a study of QDs on ATO film. Unlike ITO, the absorption of ATO at the QD emission range is negligible (see Figure 1a), which precludes energy transfer from excited QDs to the substrate as a competitive exciton quenching pathway. In addition to QD fluorescence, the ability to prepare nanoporous ATO films also enables the study of the same system by transient absorption spectroscopy. By combining transient absorption measurement and single QD fluorescence dynamics and comparing QDs on a sapphire window and nanoporous SnO_2 and ATO films, we show that, for QDs on n-type ATO film, charging-induced fast Auger relaxation is the dominant excited-state quenching pathway. The effect of QD charging on single QD blinking behavior is also examined.

RESULTS AND DISCUSSION

Ultrafast Transient Absorption and Ensemble-Averaged Fluorescence Measurements. Steady-state UV−vis absorption and emission spectra of the core/multishell (CdSe/$CdS_{3ML}ZnCdS_{2ML}ZnS_{2ML}$) quantum dots used in this study are shown in Figure 1a. From the first exciton peak position (585 nm) of the QDs, the conduction and valence band levels can be estimated to be −0.90 and 1.03 V (*vs* SCE) according to the method reported in previous studies.[22,29] The flat band potential of SnO_2 conduction band edge (E_c) depends on pH and ranges from +0.067 V (SCE) at pH = 0 to −0.35 V at pH = 7.[30,31] In this study, the conduction band edge is assumed to be −0.35 V because all measurements are done at neutral conditions. Based on the SnO_2 band gap (3.6 eV), the valence band edge (E_v) and Fermi level (E_f) are deduced to be +3.25 and +1.4 V, respectively.[31,32] As can be seen, the Fermi level of SnO_2 lays below the valence band edge of QDs. In ATO films (10% Sb in mole fraction), prepared according to published method,[31,32] the Fermi level is shifted to ~0.09 V above the E_c of SnO_2 (*i.e.*, −0.44 V), making it a n-type semiconductor.[31,32] The Fermi level is calculated from the free electron density estimated from the plasmon band absorption of the ATO in the near- to mid-IR range.[31,32] From the relative energy levels of QDs, SnO_2, and ATO (Figure 1b), the excitons in QDs on the SnO_2/ATO surface can decay by e−h recombination (with the rate k_0), electron transfer from the conduction band (CB) of the QD to the CB of SnO_2/ATO (k_{ET}), and/or hole transfer from the valence band of the QD to the filled electron levels in ATO (k_{HT}).

To examine the interaction mechanism of excited QDs on SnO_2 and ATO films, combined ensemble-averaged transient absorption (TA) and fluorescence (FL) decay measurement were conducted for QDs on sapphire windows, SnO_2 films, and ATO films. The samples were prepared by dropping water-soluble QDs with carboxylate group (−COOH)-terminated capping ligands on flat sapphire windows, nanocrystalline SnO_2, and ATO films and drying the films in air. For QD−SnO_2 and QD−ATO samples, prior to drying, the films were washed with water for 30 s to remove any weakly bound QDs. Because of the nanoporous structure of SnO_2 and ATO films, a sufficiently high loading for ensemble TA measurement can be obtained after several drop-casting−washing cycles. For QDs on sapphire windows, several cycles of QD drop-casting without washing were needed. It has to be noted that energy transfer between QDs cannot be precluded for QDs on sapphire windows where closely packed QD layers likely formed on the flat surface.[33,34] This can be seen from the fluorescence lifetime differences between the ensemble-averaged and single QD measurements (see below). Nevertheless, even with energy transfer, the lifetime of QDs on sapphire is still longer than those on other substrates. The trend of ensemble-averaged lifetimes for QDs on different substrates remains comparable; meanwhile, the comparison between TA and FL decay for each sample will not be affected since inter-QD energy transfer contributes to TA and FL decay kinetics in the same way. Therefore, we will identify the quenching mechanism based on qualitative comparison by ensemble-averaged measurements and extract the precise quenching rate and its distribution based on single QD measurement later where energy transfer between QDs can be avoided.

The transient spectra of these samples recorded after 400 nm excitation are shown in Figure S1 in the Supporting Information. These spectra show the characteristic bleach of the 1S exciton band, and the shift of higher energy exicton bands results from the formation of the 1S exciton. The decay of these features is different in these samples, which can be better seen in the comparison of the 1S exciton TA bleach recovery and FL decay kinetics for the three samples shown in Figure 1c. For better comparison, the 1S bleach recovery kinetics from TA measurement have been inverted and normalized. The TA and FL decay kinetics agree reasonably well with each other for all samples and show a trend of decreasing decay rates: ATO > SnO_2 > glass. A biexponential fit of fluorescence decay kinetics yields the amplitude-weighted average lifetime of QDs on glass (∼13 ns), SnO_2 (∼7 ns), and ATO (∼2 ns). Because the 1S exciton transient bleach signal in CdSe QDs is dominated by the state filling of the 1S conduction band electron level with negligible contribution from the holes,[35,36] the bleach recovery kinetics reflects the 1S CB electron depopulation process. The decay rate of the 1S electron TA signal is $k_{TA} = k_{ET} + k_{e-h}$, where k_{ET} is the 1S electron transfer/trapping rate and k_{e-h} is the rate of direct 1S electron−1S hole recombination. Because the transient fluorescence intensity is proportional to the concentration of both 1S electrons and holes, the fluorescence decay kinetics is given by $k_{FL} = k_{ET} + k_{e-h} + k_{HT} = k_{TA} + k_{HT}$, where k_{HT} is hole transfer/trapping rate.[29,37]

As we can see in Figure 1c, a good agreement between excited-state TA and FL decay kinetics is observed, which rules out the hole transfer/trapping/filling process for these samples. Therefore, it is the 1S electron depopulation process ($k_{ET} + k_{e-h}$) that leads to the different excited-state decay dynamics on different substrates. Compared with QDs on glass, interfacial electron transfer (with rate k_{ET}) from QDs to SnO_2/ATO leads to the faster 1S electron decay on these films, consistent with previous reports for QDs on SnO_2 films.[25−27] According to our previous study of adsorbed dye molecules on ATO films, the forward electron transfer rate (k_{ET}) from excited dye molecules to ATO does not depend on Sb doping level because conduction band states mostly remain unoccupied even after Sb doping and the electron-accepting state densities are similar for SnO_2 and ATO.[31] Therefore, it is reasonable to assume similar k_{ET} rates from QDs to SnO_2 and ATO. However, the 1S electron decays much faster for QDs on ATO than on SnO_2, suggesting an additional electron depopulation pathway for the QD−ATO sample. An additional internal/surface electron-trapping process for QDs on ATO compared with SnO_2 is unlikely since Sb doping in SnO_2 should not introduce electron-trapping states on QDs. Then the faster electron decay component on ATO films (compared with SnO_2) can only be attributed to a faster electron−hole recombination process (k_{e-h}), which contains an intrinsic radiative decay rate (k_0) and any additional nonradiative decay rate. The former can be assumed to be unchanged on these three substrates, so the significantly faster electron decay rate indicates an additional nonradiative electron−hole recombination pathway for QDs on ATO than on SnO_2.

Similar to the charging of QDs on ITO,[22,23] it is likely that QDs on ATO are also negatively charged, and we attribute the faster nonradiative electron−hole recombination process to Auger recombination in charged QDs. It is well-established now that exciton lifetimes (several nanoseconds) in charged CdSe/CdS and CdSe/ZnS core−shell QDs are shortened due to fast Auger recombination.[18,38−40] In addition to the quantum-confined electron/hole states, the nanometer-size QDs also have surface states located within the band gap due to a large surface-to-volume ratio and incomplete surface passivation.[41−44] Since the Fermi level in ATO is raised from 1.4 V (*vs* SCE) in SnO_2 (below the QDs valence band edge) to −0.44 V (1.5 V above the QDs

valence band edge and 0.5 V below the conduction band edge) after Sb doping, it is reasonable to assume that Fermi level equilibration should lead to electron transfer from ATO to empty surface midgap states in QDs, forming negatively charged QDs.[22,23] Therefore, photoexcited electron–hole pairs recombine nonradiatively by transferring energy to the surface state electron, which gets excited to a higher energy level and then relaxes back. Similar electron charging of midgap surface states in QDs has been achieved before by applying electrochemical potentials[21,45–49] and reducing agents.[50] In these charged QDs, the QD excitons decay through nonradiative multicarrier Auger recombination, which has a much shorter lifetime than radiative recombination.[18,22,38–40,51] In principle, the photoexcited holes can also recombine nonradiatively with the surface trap electrons on QDs through a hole-filling (k_{HF}) process.[21,49] However, this process should lead to faster FL decay kinetics (than TA), which is not observed experimentally (Figure 1c), suggesting that it is much slower compared with the Auger recombination rate (~2 ns). The slow hole transfer/filling is likely caused by slower hole tunneling from the CdSe core through the thick CdS/CdZnS/ZnS shell.[52,53]

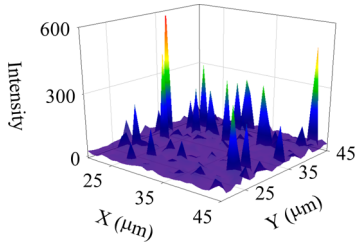

Figure 2. Raster scan fluorescence image of single QDs on SnO_2 film.

Single Quantum Dot Exciton Quenching Dynamics. To facilitate the comparison of ensemble-averaged and single QD studies, the same batch of QDs, SnO_2 films, and ATO films were used, although the films were prepared on different substates: glass coverslips and sapphire windows for single QD and ensemble-averaged measurements, respectively. To prepare samples for single QD measurement, a QD solution with a diluted concentration of ~10 pM was spin-coated on bare glass coverslips (sample 1), SnO_2 film (sample 2), and ATO films (sample 3). A typical image of single QD fluorescence on SnO_2 is shown in Figure 2. About 50 single QDs from each sample were detected, and each QD was followed for about 5 min, during which permanent photobleach was not observed. Two times associated with each detected photon, the delay time (relative to excitation pulse) and the arrival time (relative to the start of the experiment), were recorded. For each QD, the intensity trace was constructed by counting the number of photons within 50 ms arrival time windows. The delay time histograms of photons within 1 s arrival time windows were constructed and fitted to single exponential decay functions (by nonlinear least-squares fit) to obtain the lifetime trajectory.

Typical intensity and lifetime trajectories of single QDs on different substrates are shown in panels a1–a3 (1-glass, 2-SnO_2, 3-ATO) of Figure 3. The lifetime trajectory follows the intensity trajectory for QDs in all three samples, consistent with the reported positive correlation between the fluorescence intensity and lifetime of single QDs.[54–64] We attribute all points with intensity within six standard deviations of the

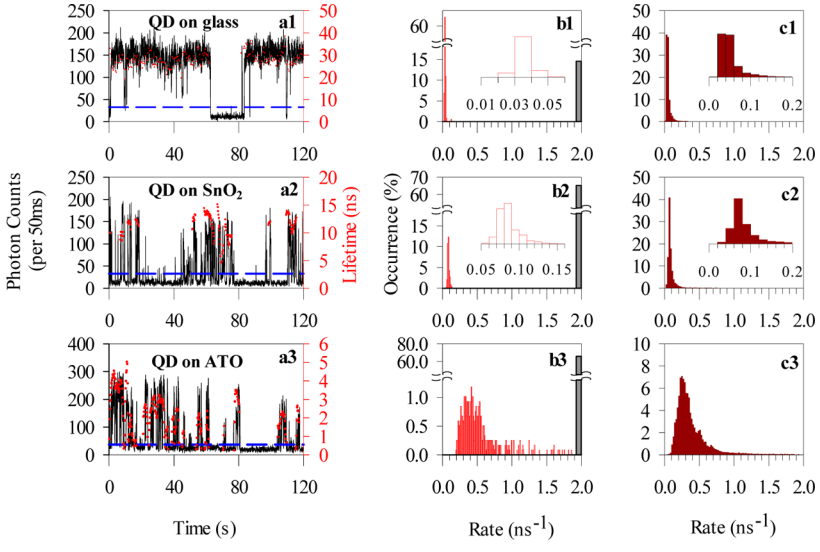

Figure 3. (a1–a3) Typical fluorescence intensity (black line) and lifetime (red dots) trajectories and (b1–b3) histograms of exciton decay rates of a representative single QD from each sample. Blue dashed lines in a1–a3 indicate the threshold separating the on- and off-states. Gray bars in b1–b3 indicate the occurrence of states with emission intensity at the background level, which has exciton quenching (EQ) rates greater than 2 ns^{-1} and lifetimes less than 0.5 ns. (c1–c3) Total histograms of on-state exciton decay rates for all (50) measured single QDs in samples 1–3.

background level to off-states and all points with higher intensities to on-states. It is clear that QDs in samples 2 and 3 have more short on-states and less long on-states compared with the QD in sample 1. The histograms of exciton decay rate (calculated as the inverse of lifetime) distributions for a representative single QD are plotted in Figure 3b1−b3. For off-states, their exciton decay rates cannot be accurately determined because of limited photon numbers and are estimated to be greater than 2 ns^{-1}. The occurrences of these states are counted and plotted with gray bars in the rate histograms as shown in Figure 3b. In sample 1 (Figure 3b1), the QD has a typical intrinsic exciton decay rate centered at 0.03 ns^{-1}. For sample 2 (b2), the QD shows a faster exciton quenching compared with QDs on glass and the peak of the distribution shifts to 0.08 ns^{-1}. QDs deposited on ATO films (b3) have the fastest exciton decay rates, centering at ~0.4 ns^{-1}. Similar distributions were observed in different QDs, and total histograms of 50 single QD on-state exciton decay rate distributions are shown in Figure 3c1−c3. The exciton fluorescence decay rates in QDs increase from sample 1 to 3, consistent with the observed trend in ensemble-averaged measurements (Figure 1c). The corresponding histograms of fluorescence intensity distributions of these samples are shown in Figure S2 in the Supporting Information. The on-state fluorescence intensity distributions shift to lower intensity from sample 1 to 3, consistent with the observed change in on-state lifetime distributions. Compared to QDs on glass, there are significant increases of the probability of off-states for QDs on SnO_2 and ATO, the reason for which will be discussed below.

The average intrinsic exciton decay rate of QDs on glass is estimated to be 0.045 ns^{-1} (Figure 1c1). The exciton quenching rate (k_{EQ}) in SnO_2 or ATO is calculated by the subtraction of exciton decay rate on SnO_2 (c2) and ATO (c3) by the intrinsic average exciton decay rate on glass (0.045 ns^{-1}). The histograms of the calculated k_{EQ} distributions for QDs on SnO_2 and ATO are depicted in Figure 4d2,d3, respectively. The average k_{EQ} in sample 2 is ~0.04 ns^{-1}, which represents the average electron transfer rate from QDs to SnO_2. This average electron transfer rate is much slower than the previously reported value for core-only CdSe QDs on SnO_2;[27] it can be attributed to the existence of ZnS shells on the core/shell QDs which act as an electron tunneling barrier to reduce the surface electron density.[52,53] The average EQ rate in sample 3 (QD−ATO) is estimated to be 0.25 ns^{-1}, which contains electron transfer rate (~0.04 ns^{-1} obtained from QD−SnO_2) and Auger recombination rate (~0.21 ns^{-1}). This Auger recombination rate is slower than the negative trion decay in electrochemically charged CdSe/CdS QDs,[18] suggesting that the Auger recombination process involving a trapped electron is slower. The full width at half-maximum of k_{EQ} distribution ($fwhm_{EQ}$) in Figure 4d is 0.05 ns^{-1} on SnO_2 and 0.22 ns^{-1} on ATO, as listed in Table 1, indicating much higher heterogeneity in the exciton quenching dynamics for QDs on ATO.

To reveal the origin of the heterogeneity of exciton quenching rates in samples 2 and 3, we calculate the average exciton quenching rate ($k_{AEQ,i}$) and associated standard deviation (SD_i) of each QD.[29,56] $k_{AEQ,i}$ is the arithmetic mean of exciton quenching rates averaged over the trajectory of QD *i*. Standard deviation, representing the extent of dynamic fluctuation of EQ rates in single each QD, is defined by the following expression

TABLE 1. Full Width at Half Maxima of Exciton Quenching Rates and Average Exciton Quenching Rate and Average Standard Deviations in Samples 2 and 3 (Calculated from the Distributions in Figure 4)

sample #	$fwhm_{EQ}$ (ns^{-1})	$fwhm_{AEQ}$ (ns^{-1})	average SD (ns^{-1})
2	0.05	0.02	0.03
3	0.22	0.20	0.08

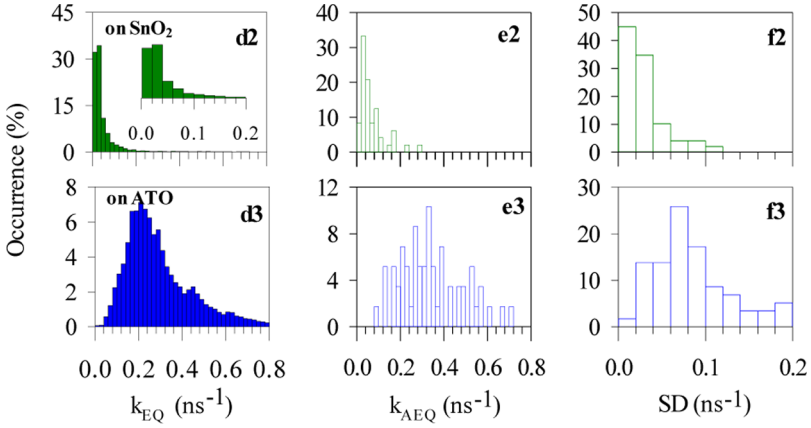

Figure 4. Histograms of total exciton quenching rates (d2,d3), average exciton decay rates (e2,e3), and standard deviations (f2,f3) for sample 2 and sample 3.

$$SD_i = \sqrt{\frac{\sum_{j=1}^{N} (k_{EQ,i}(t_j) - \langle k_{AEQ,i} \rangle)^2}{N}} \quad (1)$$

where $k_{EQ,i}(t_j)$ is the EQ rate at time t_j and the sum is over the whole trajectory. Histograms of $k_{AEQ,i}$ and SD_i for each studied QD_i (50 in total) in samples 2 and 3 are plotted in Figure 4 e2,3 and f2,3, respectively, and the averaged SD_i over 50 QDs are listed in Table 1. The distribution of k_{AEQ} reflects how the average quenching rates differ among QDs, which can be used as a rough indicator of "static" heterogeneity. The standard deviation represents how the exciton quenching rates vary with time for each QD, which provides a measure of the dynamic heterogeneity. From Figure 4e2,e3, the fwhm values of k_{AEQ} distribution ($fwhm_{AEQ}$) are calculated to be 0.02 ns^{-1} for sample 2 and 0.2 ns^{-1} for sample 3 (listed in Table 1).

For QDs on SnO_2, $fwhm_{AEQ}$ (0.02 ns^{-1}) is smaller than $fwhm_{EQ}$ (0.05 ns^{-1}) by 0.03 ns^{-1}, a value that is similar to the average SD. This result suggests that the exciton quenching rate for QDs on SnO_2 contains similar contributions of static heterogeneity and dynamic fluctuation. However, for QDs on ATO, $fwhm_{AEQ}$ is ~10-fold greater than that on SnO_2, and it is close to $fwhm_{EQ}$, indicating that static heterogeneity dominates the distribution of exciton quenching rates. Because QDs from the same batch are used for the measurements on SnO_2 and ATO films, they should have similar distribution of intrinsic exciton decay rates. On the basis of the ensemble-averaged study presented above, we attribute the faster exciton decay rate for QDs on ATO to Auger recombination caused charging of QDs. Therefore, the broad distribution of exciton quenching rates among QDs on ATO can be attributed to the distribution of Auger recombination rates, which likely indicates the heterogeneity of the number of charges and charging sites. Although the nature of surface trap states is still poorly understood, it is reasonable to assume that they are sensitive to surface chemistry and environment and can vary dramatically among QDs.

To examine the effect of charging on the statistics of the on- and off-state distributions, we have calculated the probability densities $P(t)$ of a QD in the on- or off-states for a duration time of t according to eq 2.[59,62,65−69]

$$P_i(t) = \frac{N_i(t)}{N_{i,\,total}} \times \frac{1}{\Delta t_{avg}} \quad (i = \text{on or off}) \quad (2)$$

Here, $N(t)$ is the number of "on" or "off" events with duration time of t, N_{total} is the total number of on or off events, and Δt_{avg} is the average of the time intervals to the preceding and subsequent events.

As shown in Figure 5, both $P_{on}(t)$ and $P_{off}(t)$ for single QDs from samples 1, 2, and 3 show power law distributions at short time but deviate from this at longer time,

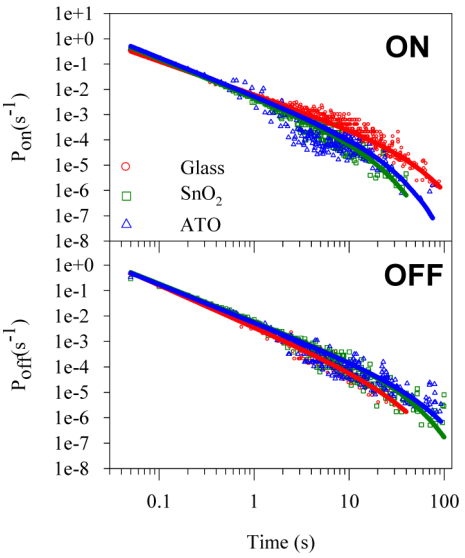

Figure 5. Probability density distributions of (a) on-states (P_{on}) and (b) off-states (P_{off}) as a function of on (off) time intervals, constructed from 50 QDs from sample 1 (red circle), sample 2 (green square), and sample 3 (blue triangle). The solid lines are the best fits according to eq 3.

TABLE 2. Fitting Parameters of $P_{on}(t)$ and $P_{off}(t)$ for All Single QDs from Samples 1, 2, and 3

sample #	m_{on}	$1/\Gamma_{on}$ (s)	m_{off}	$1/\Gamma_{off}$ (s)
1	1.32 ± 0.04	36.5 ± 4.3	1.65 ± 0.05	25.1 ± 3.9
2	1.52 ± 0.06	12.0 ± 1.5	1.49 ± 0.04	27.4 ± 2.9
3	1.51 ± 0.08	16.4 ± 3.4	1.50 ± 0.07	42.6 ± 3.9

similar to results reported for free QDs and QD−electron acceptor complexes.[59,62,65−69] These $P(t)$ distributions can be fit by a truncated power law:

$$P_i(t) = B_i t^{-m_i} \exp(-\Gamma_i t) \quad (i = \text{on or off}) \quad (3)$$

where B is the amplitude, m the power law exponent, and Γ the saturation rate. The fitting parameters are listed in Table 2. Noticeable differences between QDs on glass and on SnO_2/ATO are observed: compared to QDs on glass, QDs on SnO_2 have larger m_{on} and Γ_{on} as well as smaller m_{off} and Γ_{off}. This suggests that electron transfer from QDs to SnO_2 reduces probability densities of long on events and increases probability densities of long off events, which is consistent with the findings of previous works.[54−56] For QDs on ATO films, the probabilities of "on" time and "off" time remain similar to QDs on SnO_2 except for slightly decreased Γ_{off}. This indicates that the charging of QDs on ATO does not significantly affect the occurrence and the probability density distributions of the on- and off-states compared with SnO_2.

Although the blinking of QDs was observed more than 10 years ago, its origin remains an intensely debated subject.[21,70−74] The on/off-states of QDs are commonly ascribed to charged/neutral QDs. Once a carrier (electron or hole) is ejected from the QD core to surface traps and surrounding matrix, the QD is

charged and a much faster (compared with radiative recombination) multicarrier Auger recombination process annihilates the subsequent photoexcited e−h pair nonradiatively, leading to off-states with reduced emission intensity and shortened lifetime.[57,70,71] QDs can return to on-states (and become bright) again when they are neutralized. However, recent observations of biexciton emission (which should have lower emission quantum yield than a positive trion), negative trion emission,[17−19] and size-independent off-state lifetime in single QDs have led to the re-examination of the nature of the off-state.[18,72,73] Many combined electrochemistry and single QD measurements show that negatively charged QDs can still be emissive although with lower emission intensity and lifetime.[17−19,21] Our previous study of QD−hole acceptor complexes shows that negatively charge QDs generated by hole transfer to the acceptor are also emissive, showing an enhanced probability of low emission ("gray") states.[29]

For QDs on ATO, the Fermi level equilibration leads to negatively charged QDs, a condition that is similar to QDs under negative external bias. From the observed exciton quenching rate (0.25 ns^{-1}), the emission quantum yield can be calculated to be 15% assuming the same e−h radiative recombination rate as QDs on glass (0.045 ns^{-1}). The emission from these charged QDs is weaker than neutral QD but still high enough to be observed and attributed to on-state or gray state, consistent with the experimental observation. Therefore, compared with QDs on SnO_2, the charging of QDs on ATO, which shortens exciton lifetime due to nonradiative Auger recombination, does not increase the off-state or decrease the on-state probability densities. It appears that the charge state of the QD remains unchanged after the Auger recombination process. Both the observed lifetime and blinking dynamics of single QDs on ATO are consistent with experimental observations of negatively charged QDs.[17−19,21]

The observed shortened on-state fluorescence lifetime of QDs on ATO is similar to that previously reported for the similar QDs on ITO, suggesting that fast Auger recombination due to negatively charged QD is also a likely quenching mechanism in the latter. However, the blinking behaviors in these systems are quite different. It has been reported that single QDs in contact with electron-donating molecules or (n-doped) ITO substrates show suppressed blinking dynamics,[22,75] which was attributed to the efficient removal of the extra holes in the off-state by the electrons from molecules or ITO, reducing the off-state probability. According to this model, the different blinking dynamics on ATO and ITO films likely indicates different hole removal rates for QDs on these films. This difference may be caused by the lower free electron density in ATO, which is typically ∼10-fold or more lower than ITO.[22,32]

CONCLUSIONS

The exciton quenching dynamics of core/multishell ($CdSe/CdS_{3ML}ZnCdS_{2ML}ZnS_{2ML}$) quantum dots deposited on glass, SnO_2, and ATO films have been studied by transient absorption spectroscopy and ensemble-averaged and single QD fluorescence spectroscopy. The exciton quenching rates on these substrates increase from glass to SnO_2 to ATO. Comparison of ensemble-averaged TA and FL decay kinetics shows that these kinetics agree with each other, reflecting the decay the 1S electron population. Compared to QDs on glass, the faster exciton quenching on SnO_2 is attributed to electron transfer from the excited QDs to SnO_2. Because similar electron transfer rates are expected on SnO_2 and ATO, the faster exiton quenching rate for QDs on ATO suggests additional electron decay pathway and is attributed to fast Auger recombination in charged QDs formed by Fermi level equilibration between QDs and n-doped ATO films. Single QDs on all substrates show correlated fluorescence intensity and emission lifetime (*i.e.*, blinking dynamics). The blinking dynamics of QDs on ATO and SnO_2 are similar, showing similar on and off time probability densities. Compared to QDs on glass, they show decreased probabilities of long on-states and increased probabilities of long off-states. For QDs on SnO_2, we observe comparable contributions of static and dynamic heterogeneity to the total distribution of exciton quenching rates. On ATO surfaces, the static heterogeneity is greatly increased compared to QDs on SnO_2, indicating a large heterogeneity of Auger recombination rates in charged QDs, which is likely caused by a distribution of the number of charges and/or charging sites on the QD surface.

METHODS

Sample Preparation. Water-soluble $CdSe/CdS_{3ML}ZnCdS_{2ML}ZnS_{2ML}$ core/shell QDs with the first exciton peak at 585 nm were obtained from Ocean NanoTech, LLC, USA. Colloidal ATO was synthesized according to a published procedure.[31,32] Briefly, 30 g (∼85 mmol) of $SnCl_4 \cdot 5H_2O$ (98%, from Aldrich) was dissolved in 500 mL of H_2O (Millipore, 18.3 MΩ/cm), to which a solution of $SbCl_3$ (98%, from Aldrich) dissolved in 20 mL of HCl (37 wt %) was added dropwise in an ice bath under rapid stirring. The doping level was controlled by the amount of $SbCl_3$ solution added, and two samples with Sb/Sn molar ratios of 0:1 and 0.1:1 (referred to as SnO_2 and 10% ATO, respectively) were prepared. The resulting clear colorless solution was stirred for 30 min before aqueous ammonia (25%) was added to adjust the pH to 3.5−4.0 and was allowed to settle overnight in the dark. The precipitate was washed at least three times with water and resuspended in water. The suspension was adjusted to pH 9.5−10, stirred vigorously overnight, and dialyzed against 10 L of aqueous ammonia at pH 10 to produce clear ATO colloidal solution. The ATO colloidal solution was refluxed for 4 h. This colloid (120 mL) was poured into an autoclave and heated at 150 °C for 1 h and at 270 °C for 16 h. The colloid was then concentrated to 60 mL.

Five milliliters of the solution and 2 drops of TritonX-100 (from Aldrich) were mixed and stirred for 1 day. The resulting solution was cast onto sapphire windows, dried in air, and then baked at 400 °C for 1 h in an oven to produce nanoporous crystalline thin films. A detailed characterization of the ATO films prepared in our laboratory by X-ray diffraction, scanning electron microscopy, and FTIR were described in a previous publication.[31,32]

Ensemble-Averaged Measurements. Ultrafast and nanosecond transient absorption experiment setup has been described previously.[29,56] During the data collection, samples were constantly translated to avoid permanent photodamage. Ensemble-averaged fluorescence lifetimes of the same samples were measured. The emission was detected by a microchannel plate photomultiplier tube (Hamamatsu R3809U-51), whose output was amplified and analyzed by a TCSPC board (Becker & Hickel SPC 600).

Single Molecule/Particle Fluorescence Spectroscopy. The single QD fluorescence decay was measured using a home-built scanning confocal microscope. Femtosecond laser pulses (~100 fs) with a repetition rate of 80 MHz were generated with a mode-locked Ti:sapphire laser (Tsunami oscillator pumped by a 10 W Millennia Pro, Spectra-Physics). The output centered at 1000 nm was passed through a pulse picker (Conoptics, USA) to reduce the repetition rate by a factor of 9. Excitation pulses at 500 nm were generated by second-harmonic generation of the 1000 nm pulses in a BBO crystal. The excitation beam (~200 nW) was focused through an objective (100×, N.A. 1.4, oil immersion, Olympus) down to a diffraction-limited spot on the sample, which was spin-coated onto glass coverslips and placed on a piezo scanner (Mad City Laboratories). The resulting epi-fluorescence from the sample was detected by an avalanche photodiode (APD, PerkinElmer SPCM-AQR-14). The APD output was analyzed by a time-correlated single photon counting (TCSPC) board (Becker & Hickel SPC 600). The instrument response function for the fluorescence lifetime measurement had a full width at half-maximum of ~500 ps.

Conflict of Interest: The authors declare no competing financial interest.

Acknowledgment. The authors gratefully acknowledge the financial support from the National Science Foundation (CHE-0848556 and CHE-1212907).

Supporting Information Available: Ensemble-averaged transient absorption spectra. This material is available free of charge *via* the Internet at http://pubs.acs.org.

REFERENCES AND NOTES

1. Yu, W. W.; Qu, L. H.; Guo, W. Z.; Peng, X. G. Experimental Determination of the Extinction Coefficient of CdTe, CdSe, and CdS Nanocrystals. *Chem. Mater.* **2003**, *15*, 2854–2860.
2. Zhu, H.; Song, N.; Lian, T. Wave Function Engineering for Ultrafast Charge Separation and Slow Charge Recombination in Type II Core/Shell Quantum Dots. *J. Am. Chem. Soc.* **2011**, *133*, 8762–8771.
3. Zhu, H.; Lian, T. Wavefunction Engineering in Quantum Confined Semiconductor Nanoheterostructures for Efficient Charge Separation and Solar Energy Conversion. *Energy Environ. Sci.* **2012**, *5*, 9406–9418.
4. Alivisatos, A. P. Semiconductor Clusters, Nanocrystals, and Quantum Dots. *Science* **1996**, *271*, 933–937.
5. Bruchez, M., Jr.; Moronne, M.; Gin, P.; Weiss, S.; Alivisatos, A. Semiconductor Nanocrystals as Fluorescent Biological Labels. *Science* **1998**, *281*, 2013–2016.
6. Chan, W. C. W.; Nie, S. M. Quantum Dot Bioconjugates for Ultrasensitive Nonisotopic Detection. *Science* **1998**, *281*, 2016–2018.
7. Colvin, V. L.; Schlamp, M. C.; Alivisatos, A. P. Light-Emitting Diodes Made from Cadmium Selenide Nanocrystals and a Semiconducting Polymer. *Nature* **1994**, *370*, 354–357.
8. Coe, S.; Woo, W.-K.; Bawendi, M.; Bulovic, V. Electroluminescence from Single Monolayers of Nanocrystals in Molecular Organic Devices. *Nature* **2002**, *420*, 800–803.
9. Konstantatos, G.; Howard, I.; Fischer, A.; Hoogland, S.; Clifford, J.; Klem, E.; Levina, L.; Sargent, E. H. Ultrasensitive Solution-Cast Quantum Dot Photodetectors. *Nature* **2006**, *442*, 180–183.
10. Huynh, W. U.; Dittmer, J. J.; Alivisatos, A. P. Hybrid Nanorod-Polymer Solar Cells. *Science* **2002**, *295*, 2425–2427.
11. Robel, I.; Subramanian, V.; Kuno, M.; Kamat, P. V. Quantum Dot Solar Cells. Harvesting Light Energy with CdSe Nanocrystals Molecularly Linked to Mesoscopic TiO_2 Films. *J. Am. Chem. Soc.* **2006**, *128*, 2385–2393.
12. Zhu, H.; Song, N.; Lv, H.; Hill, C. L.; Lian, T. Near Unity Quantum Yield of Light-Driven Redox Mediator Reduction and Efficient H2 Generation Using Colloidal Nanorod Heterostructures. *J. Am. Chem. Soc.* **2012**, *134*, 11701–11708.
13. Greenham, N. C.; Peng, X.; Alivisatos, A. P. Charge Separation and Transport in Conjugated-Polymer/Semiconductor-Nanocrystal Composites Studied by Photoluminescence Quenching and Photoconductivity. *Phys. Rev. B* **1996**, *54*, 17628–17637.
14. Klem, E. J. D.; MacNeil, D. D.; Levina, L.; Sargent, E. H. Solution Processed Photovoltaic Devices with 2% Infrared Monochromatic Power Conversion Efficiency: Performance Optimization and Oxide Formation. *Adv. Mater.* **2008**, *20*, 3433–3439.
15. Leschkies, K. S.; Beatty, T. J.; Kang, M. S.; Norris, D. J.; Aydil, E. S. Solar Cells Based on Junctions between Colloidal Pbse Nanocrystals and Thin ZnO Films. *ACS Nano* **2009**, *3*, 3638–3648.
16. Rivest, J. B.; Swisher, S. L.; Fong, L.-K.; Zheng, H.; Alivisatos, A. P. Assembled Monolayer Nanorod Heterojunctions. *ACS Nano* **2011**, *5*, 3811–3816.
17. Jha, P. P.; Guyot-Sionnest, P. Photoluminescence Switching of Charged Quantum Dot Films. *J. Phys. Chem. C* **2007**, *111*, 15440–15445.
18. Jha, P. P.; Guyot-Sionnest, P. Trion Decay in Colloidal Quantum Dots. *ACS Nano* **2009**, *3*, 1011–1015.
19. Jha, P. P.; Guyot-Sionnest, P. Electrochemical Switching of the Photoluminescence of Single Quantum Dots. *J. Phys. Chem. C* **2010**, *114*, 21138–21141.
20. White, M. A.; Weaver, A. L.; Beaulac, R. M.; Gamelin, D. R. Electrochemically Controlled Auger Quenching of Mn^{2+} Photoluminescence in Doped Semiconductor Nanocrystals. *ACS Nano* **2011**, *5*, 4158–4168.
21. Galland, C.; Ghosh, Y.; Steinbruck, A.; Sykora, M.; Hollingsworth, J. A.; Klimov, V. I.; Htoon, H. Two Types of Luminescence Blinking Revealed by Spectroelectrochemistry of Single Quantum Dots. *Nature* **2011**, *479*, 203–207.
22. Jin, S.; Song, N.; Lian, T. Suppressed Blinking Dynamics of Single QDs on ITO. *ACS Nano* **2010**, *4*, 1545–1552.
23. Yalcin, S. E.; Yang, B.; Labastide, J. A.; Barnes, M. D. Electrostatic Force Microscopy and Spectral Studies of Electron Attachment to Single Quantum Dots on Indium Tin Oxide Substrates. *J. Phys. Chem. C* **2012**, *116*, 15847–15853.
24. Qin, W.; Guyot-Sionnest, P. Evidence for the Role of Holes in Blinking: Negative and Oxidized CdSe/CdS Dots. *ACS Nano* **2012**, *6*, 9125–9132.
25. Leventis, H. C.; O'Mahony, F.; Akhtar, J.; Afzaal, M.; O'Brien, P.; Haque, S. A. Transient Optical Studies of Interfacial Charge Transfer at Nanostructured Metal Oxide/PbS Quantum Dot/Organic Hole Conductor Heterojunctions. *J. Am. Chem. Soc.* **2010**, *132*, 2743–2750.
26. Pijpers, J. J. H.; Koole, R.; Evers, W. H.; Houtepen, A. J.; Boehme, S.; de Mello Donegaì, C.; Vanmaekelbergh, D.; Bonn, M. Spectroscopic Studies of Electron Injection in Quantum Dot Sensitized Mesoporous Oxide Films. *J. Phys. Chem. C* **2010**, *114*, 18866–18873.
27. Tvrdy, K.; Frantsuzov, P. A.; Kamat, P. V. Photoinduced Electron Transfer from Semiconductor Quantum Dots to Metal Oxide Nanoparticles. *Proc. Natl. Acad. Sci. U.S.A.* **2011**, *108*, 29–34.
28. Hossain, M. A.; Jennings, J. R.; Koh, Z. Y.; Wang, Q. Carrier Generation and Collection in CdS/CdSe-Sensitized SnO_2 Solar Cells Exhibiting Unprecedented Photocurrent Densities. *ACS Nano* **2011**, *5*, 3172–3181.

29. Song, N.; Zhu, H.; Jin, S.; Lian, T. Hole Transfer from Single Quantum Dots. *ACS Nano* **2011**, *5*, 8750–8759.
30. Ai, X.; Anderson, N. A.; Guo, J. C.; Lian, T. Q. Electron Injection Dynamics of Ru Polypyridyl Complexes on SnO_2 Nanocrystalline Thin Films. *J. Phys. Chem. B* **2005**, *109*, 7088–7094.
31. Guo, J. C.; She, C. X.; Lian, T. Q. Ultrafast Electron Transfer between Molecule Adsorbate and Antimony Doped Tin Oxide (ATO) Nanoparticles. *J. Phys. Chem. B* **2005**, *109*, 7095–7102.
32. Guo, J. C.; She, C. X.; Lian, T. Q. Ultrafast Electron Transfer between Conjugated Polymer and Antimony-Doped Tin Oxide (ATO) Nanoparticles. *J. Phys. Chem. C* **2008**, *112*, 4761–4766.
33. Crooker, S. A.; Hollingsworth, J. A.; Tretiak, S.; Klimov, V. I. Spectrally Resolved Dynamics of Energy Transfer in Quantum-Dot Assemblies: Towards Engineered Energy Flows in Artificial Materials. *Phys. Rev. Lett.* **2002**, *89*, 186802.
34. Kagan, C. R.; Murray, C. B.; Nirmal, M.; Bawendi, M. G. Electronic Energy Transfer in CdSe Quantum Dot Solids. *Phys. Rev. Lett.* **1996**, *76*, 1517–1520.
35. Klimov, V. I. Optical Nonlinearities and Ultrafast Carrier Dynamics in Semiconductor Nanocrystals. *J. Phys. Chem. B* **2000**, *104*, 6112–6123.
36. Klimov, V. I. Spectral and Dynamical Properties of Multiexcitons in Semiconductor Nanocrystals. *Annu. Rev. Phys. Chem.* **2007**, *58*, 635–673.
37. Knowles, K. E.; McArthur, E. A.; Weiss, E. A. A Multi-Timescale Map of Radiative and Nonradiative Decay Pathways for Excitons in CdSe Quantum Dots. *ACS Nano* **2011**, *5*, 2026–2035.
38. Goìmez, D. E.; van Embden, J.; Mulvaney, P.; Ferneìe, M. J.; Rubinsztein-Dunlop, H. Exciton−Trion Transitions in Single CdSe−CdS Core−Shell Nanocrystals. *ACS Nano* **2009**, *3*, 2281–2287.
39. Spinicelli, P.; Buil, S.; Quelin, X.; Mahler, B.; Dubertret, B.; Hermier, J. P. Bright and Grey States in CdSe−CdS Nanocrystals Exhibiting Strongly Reduced Blinking. *Phys. Rev. Lett.* **2009**, *102*, 136801–4.
40. Yalcin, S. E.; Labastide, J. A.; Sowle, D. L.; Barnes, M. D. Spectral Properties of Multiply Charged Semiconductor Quantum Dots. *Nano Lett.* **2011**, *11*, 4425–4430.
41. Sercel, P. C.; Efros, A. L.; Rosen, M. Intrinsic Gap States in Semiconductor Nanocrystals. *Phys. Rev. Lett.* **1999**, *83*, 2394–2397.
42. Fu, H.; Zunger, A. Inp Quantum Dots: Electronic Structure, Surface Effects, and the Redshifted Emission. *Phys. Rev. B* **1997**, *56*, 1496–1508.
43. Hässelbarth, A.; Eychmüller, A.; Weller, H. Detection of Shallow Electron Traps in Quantum Sized CdS by Fluorescence Quenching Experiments. *Chem. Phys. Lett.* **1993**, *203*, 271–276.
44. Lifshitz, E.; Dag, I.; Litvitn, I. D.; Hodes, G. Optically Detected Magnetic Resonance Study of Electron/Hole Traps on CdSe Quantum Dot Surfaces. *J. Phys. Chem. B* **1998**, *102*, 9245–9250.
45. Wang, C.; Shim, M.; Guyot-Sionnest, P. Electrochromic Nanocrystal Quantum Dots. *Science* **2001**, *291*, 2390–2392.
46. Weaver, A. L.; Gamelin, D. R. Photoluminescence Brightening *via* Electrochemical Trap Passivation in ZnSe and Mn^{2+}-Doped ZnSe Quantum Dots. *J. Am. Chem. Soc.* **2012**, *134*, 6819–6825.
47. Schäfer, S.; Wang, Z.; Kipp, T.; Mews, A. Fluorescence Modulation of Single CdSe Nanowires by Charge Injection through the Tip of an Atomic-Force Microscope. *Phys. Rev. Lett.* **2011**, *107*, 137403.
48. Wang, C.; Wehrenberg, B. L.; Woo, C. Y.; Guyot-Sionnest, P. Light Emission and Amplification in Charged CdSe Quantum Dots. *J. Phys. Chem. B* **2004**, *108*, 9027–9031.
49. Gooding, A. K.; Gómez, D. E.; Mulvaney, P. The Effects of Electron and Hole Injection on the Photoluminescence of CdSe/CdS/ZnS Nanocrystal Monolayers. *ACS Nano* **2008**, *2*, 669–676.
50. Bang, J.; Chon, B.; Won, N.; Nam, J.; Joo, T.; Kim, S. Spectral Switching of Type-II Quantum Dots by Charging. *J. Phys. Chem. C* **2009**, *113*, 6320–6323.
51. Klimov, V. I.; Mikhailovsky, A. A.; McBranch, D. W.; Leatherdale, C. A.; Bawendi, M. G. Quantization of Multiparticle Auger Rates in Semiconductor Quantum Dots. *Science* **2000**, *287*, 1011–1013.
52. Zhu, H.; Song, N.; Lian, T. Controlling Charge Separation and Recombination Rates in CdSe/ZnS Type I Core−Shell Quantum Dots by Shell Thicknesses. *J. Am. Chem. Soc.* **2010**, *132*, 15038–15045.
53. Zhu, H.; Song, N.; Rodríguez-Córdoba, W.; Lian, T. Wave Function Engineering for Efficient Extraction of up to Nineteen Electrons from One CdSe/CdS Quasi-Type II Quantum Dot. *J. Am. Chem. Soc.* **2012**, *134*, 4250–4257.
54. Jin, S.; Lian, T. Electron Transfer Dynamics from Single CdSe/ZnS Quantum Dots to TiO_2 Nanoparticles. *Nano Lett.* **2009**, *9*, 2448–2454.
55. Jin, S.; Hsiang, J.-C.; Zhu, H.; Song, N.; Dickson, R. M.; Lian, T. Correlated Single Quantum Dot Blinking and Interfacial Electron Transfer Dynamics. *Chem. Sci.* **2010**, *1*, 519–526.
56. Song, N.; Zhu, H.; Jin, S.; Zhan, W.; Lian, T. Poisson-Distributed Electron-Transfer Dynamics from Single Quantum Dots to C60 Molecules. *ACS Nano* **2011**, *5*, 613–621.
57. Efros, A. L.; Rosen, M. Random Telegraph Signal in the Photoluminescence Intensity of a Single Quantum Dot. *Phys. Rev. Lett.* **1997**, *78*, 1110–1113.
58. Schlegel, G.; Bohnenberger, J.; Potapova, I.; Mews, A. Fluorescence Decay Time of Single Semiconductor Nanocrystals. *Phys. Rev. Lett.* **2002**, *88*, 137401.
59. Kuno, M.; Fromm, D. P.; Johnson, S. T.; Gallagher, A.; Nesbitt, D. J. Modeling Distributed Kinetics in Isolated Semiconductor Quantum Dots. *Phys. Rev. B* **2003**, *67*, 125304.
60. Fisher, B. R.; Eisler, H. J.; Stott, N. E.; Bawendi, M. G. Emission Intensity Dependence and Single-Exponential Behavior in Single Colloidal Quantum Dot Fluorescence Lifetimes. *J. Phys. Chem. B* **2004**, *108*, 143–148.
61. Issac, A.; von Borczyskowski, C.; Cichos, F. Correlation between Photoluminescence Intermittency of CdSe Quantum Dots and Self-Trapped States in Dielectric Media. *Phys. Rev. B* **2005**, *71*, 161302.
62. Tang, J.; Marcus, R. A. Determination of Energetics and Kinetics from Single-Particle Intermittency and Ensemble-Averaged Fluorescence Intensity Decay of Quantum Dots. *J. Chem. Phys.* **2006**, *125*, 044703.
63. Issac, A.; Jin, S. Y.; Lian, T. Q. Intermittent Electron Transfer Activity from Single CdSe/ZnS Quantum Dots. *J. Am. Chem. Soc.* **2008**, *130*, 11280.
64. Montiel, D.; Yang, H. Observation of Correlated Emission Intensity and Polarization Fluctuations in Single CdSe/ZnS Quantum Dots. *J. Phys. Chem. A* **2008**, *112*, 9352–9355.
65. Shimizu, K. T.; Neuhauser, R. G.; Leatherdale, C. A.; Empedocles, S. A.; Woo, W. K.; Bawendi, M. G. Blinking Statistics in Single Semiconductor Nanocrystal Quantum Dots. *Phys. Rev. B* **2001**, *63*, 205316.
66. Verberk, R.; van Oijen, A. M.; Orrit, M. Simple Model for the Power-Law Blinking of Single Semiconductor Nanocrystals. *Phys. Rev. B* **2002**, *66*, 233202.
67. Tang, J.; Marcus, R. A. Single Particle *versus* Ensemble Average: From Power-Law Intermittency of a Single Quantum Dot to Quasistretched Exponential Fluorescence Decay of an Ensemble. *J. Chem. Phys.* **2005**, *123*, 204511.
68. Tang, J.; Marcus, R. A. Diffusion-Controlled Electron Transfer Processes and Power-Law Statistics of Fluorescence Intermittency of Nanoparticles. *Phys. Rev. Lett.* **2005**, *95*, 107401.
69. Jau, T.; Marcus, R. A. Mechanisms of Fluorescence Blinking in Semiconductor Nanocrystal Quantum Dots. *J. Chem. Phys.* **2005**, *123*, 54704-1−12.
70. Nirmal, M.; Dabbousi, B. O.; Bawendi, M. G.; Macklin, J. J.; Trautman, J. K.; Harris, T. D.; Brus, L. E. Fluorescence Intermittency in Single Cadmium Selenide Nanocrystals. *Nature* **1996**, *383*, 802–804.
71. Kuno, M.; Fromm, D. P.; Hamann, H. F.; Gallagher, A.; Nesbitt, D. J. "On"/"Off" Fluorescence Intermittency of Single Semiconductor Quantum Dots. *J. Chem. Phys.* **2001**, *115*, 1028–1040.

72. Rosen, S.; Schwartz, O.; Oron, D. Transient Fluorescence of the Off State in Blinking CdSe/CdS/ZnS Semiconductor Nanocrystals Is Not Governed by Auger Recombination. *Phys. Rev. Lett.* **2010**, *104*, 157404.
73. Zhao, J.; Nair, G.; Fisher, B. R.; Bawendi, M. G. Challenge to the Charging Model of Semiconductor-Nanocrystal Fluorescence Intermittency from Off-State Quantum Yields and Multiexciton Blinking. *Phys. Rev. Lett.* **2010**, *104*, 157403.
74. Frantsuzov, P.; Kuno, M.; Janko, B.; Marcus, R. A. Universal Emission Intermittency in Quantum Dots, Nanorods and Nanowires. *Nat. Phys.* **2008**, *4*, 519–522.
75. Hohng, S.; Ha, T. Near-Complete Suppression of Quantum Dot Blinking in Ambient Conditions. *J. Am. Chem. Soc.* **2004**, *126*, 1324–1325.